Surface Chemistry

DOI: 10.1002/anie.201207566

Coverage-Induced Hydrogen Transfer on ZnO Surfaces: From Ideal to Real Systems**

Heshmat Noei, Federico Gallino, Lanying Jin, Jianli Zhao, Cristiana Di Valentin, and Yuemin Wang**

Hydrogen transfer on metal oxide surfaces is a fundamental process in heterogeneous catalysis and photocatalysis. In general, oxide surfaces expose coordinately unsaturated (CUS) oxygen and metal ions which serve as Lewis base and acid sites, respectively. The cooperative interplay between these two CUS centers plays a crucial role in the activation of surface reactions involving hydrogen transfer.[1] For example, it has been found that H_2O can be adsorbed both molecularly and dissociatively at metal cations on oxide surfaces.[2–4] The (partial) dissociation of H_2O is triggered by hydrogen-bond interactions, which leads to hydrogen transfer onto adjacent O sites, thus forming hydroxy groups.[5–8] Water dimerization at full monolayer coverage has been previously shown to induce proton dissociation on a stoichiometric MgO surface.[6] Water-mediated Grotthuss-like proton diffusion[9] was also reported on ZnO and TiO_2 surfaces.[10,11]

The chemistry of NH_3 on metal oxide surfaces is of particular importance, because ammonia is a prototype molecule for investigating the acid–base properties of oxide surfaces. Herein, we present a combined experimental and theoretical study of NH_3 adsorption on ZnO surfaces of both single crystals and powder particles. By the application of novel ultrahigh vacuum (UHV) infrared spectroscopy we were able to obtain high-quality IR data on polycrystalline ZnO powder samples which reveal that NH_3 interacts with ZnO in a complicated manner and forms different species. A comprehensive and atomistic picture of the interfacial chemistry of NH_3 on ZnO has been established by the so-called surface-science approach,[12,13] which is based on a systematic study of well-characterized ZnO single-crystal surfaces by high-resolution electron energy loss spectroscopy (HREELS) and thermal desorption spectroscopy (TDS) in conjunction with accurate density functional theoretical (DFT) calculations. The experimental and theoretical results demonstrate that, when at low coverage, NH_3 prefers to adsorb as an intact molecule, whereas at full monolayer (ML) every second NH_3 molecule is dissociated on the perfect nonpolar ZnO($10\bar{1}0$) surface, thus yielding a mixed adlayer of NH_3, NH_2, and OH species. The unexpected hydrogen transfer between adsorbed NH_3 and surface O atoms is a consequence of the complex interplay of multiple factors, including H-bonding, steric repulsion, and pK_a.

Figure 1 presents UHV-FTIR spectra recorded after NH_3 adsorption on clean, adsorbate-free ZnO nanoparticles at 100 K and subsequent heating to higher temperatures. The

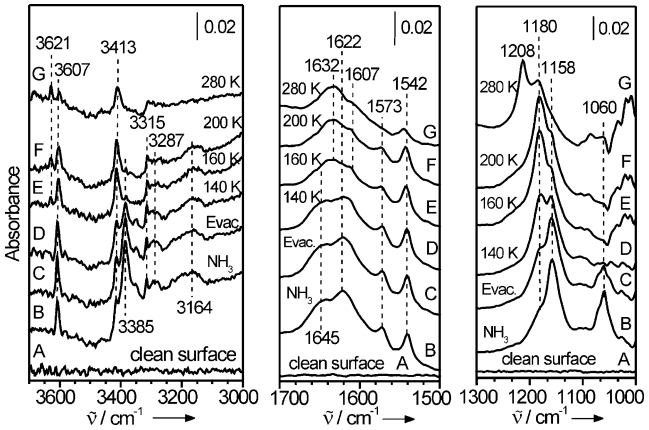

Figure 1. UHV-FTIR spectra obtained after exposing A) the clean ZnO nanoparticles to B) NH_3 (1×10^{-4} mbar) at 100 K, and then C) Under UHV at 100 K for 30 min, followed by heating to the indicated temperatures: D) 140 K, E) 160 K, F) 200 K, G) 280 K.

adsorption of NH_3 on ZnO is of a complex nature and leads to the appearance of a large number of IR bands originating from the coexistence of various NH_3-related species, as discussed in detail below (see Table 1). The temperature-dependent IR data provide further information about the thermal stability of different species adsorbed on ZnO. At high frequencies a dominating IR band is observed at 3607 cm^{-1}, which remains unchanged in intensity during heating up to 200 K. This band is characteristic of an isolated OH group on ZnO,[14] thus indicating hydrogen transfer from adsorbed NH_3 to an adjacent surface oxygen atom. After

[*] Dr. H. Noei,[#] [+] L. Jin,[+] Dr. J. Zhao, Dr. Y. Wang
Lehrstuhl für Technische Chemie and Lehrstuhl für Physikalische Chemie I, Ruhr-Universität Bochum
44780 Bochum (Germany)
E-mail: wang@pc.rub.de
Dr. F. Gallino,[$] [+] Prof. Dr. C. Di Valentin
Dipartimento di Scienza dei Materiali, Università di Milano-Bicocca
via R. Cozzi 53, 20125 Milano (Italy)
E-mail: cristiana.divalentin@mater.unimib.it
[$] Current address: SAES Getters S.p.A.
20020 Lainate (Italy)
[#] Current address: Deutsches Elektronen-Synchrotron DESY
22607 Hamburg (Germany)
[+] These authors contributed equally to this work.

[**] This work was supported by the German Research Foundation (DFG) within SFB 558 and by the CARIPLO Foundation through an Advanced Materials Grant 2009. We are grateful to Prof. P. Ugliengo and Dr. B. Civalleri for useful discussions and to CILEA for computational resources.

Supporting information for this article is available on the WWW under http://dx.doi.org/10.1002/anie.201207566.

further annealing to higher temperatures, the 3607 cm^{-1} band decreases significantly in intensity and disappears almost entirely at ca. 280 K (Figure 1 a, curve G). We can definitively rule out the recombination desorption of hydroxy groups as H_2O, which does not occur on ZnO at temperatures lower than 300 K.[14,15] This finding reveals the coverage-dependent back-transfer of hydrogen from surface O atoms to the NH_2 species, as demonstrated below.

Because of the great complexity of real oxide powder samples, to understand NH_3 chemistry on ZnO at an atomic level it is necessary to obtain corresponding experimental and theoretical data on well-defined ZnO surfaces. It is known that polycrystalline ZnO nanoparticles are dominated by a nonpolar mixed-terminated $(10\bar{1}0)$ surface,[16] which is the energetically most stable and exposes undercoordinated Zn–O ion pairs that act as both Lewis acid and base sites.[17] Figure 2 a shows the TDS data recorded after exposing the $ZnO(10\bar{1}0)$ surface to NH_3 at 100 K. Four desorption peaks of NH_3 are observed at 390, 280, 175, and 140 K, which indicates the presence of various adsorbate states, denoted as α_1, α_2, β, and γ. The β state is not saturated and slightly shifts from 175 K to 180 K with increasing NH_3 exposure (Figure 2 a, inset). This is characteristic of zero-order desorption kinetics

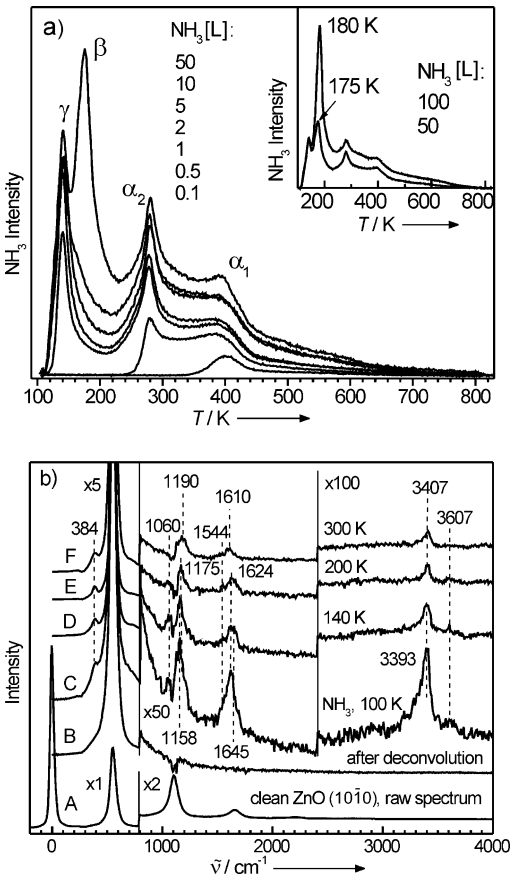

Figure 2. a) TDS data of NH_3 for varying degrees of NH_3 exposure on $ZnO(10\bar{1}0)$ at 100 K. The heating rate was 1 K s^{-1}. b) HREELS data recorded after exposing the $ZnO(10\bar{1}0)$ surface (curves A and B) to 100 L of NH_3 at 100 K and subsequently annealing to the indicated temperatures (curves C–F). Curves B–F were obtained after Fourier deconvolution to remove surface phonons.

for multilayer NH_3 species bonded to the first layer NH_3 by intermolecular H bonds. The more strongly bound α_2 and α_1 phases are attributed to the full- and sub-monolayer NH_3 desorption on $ZnO(10\bar{1}0)$, respectively. Assuming a pre-exponential factor of 10^{13} s^{-1} and first-order kinetics, activation energies of 0.77 and 1.08 eV for the desportion of α_2 and α_1 NH_3, respectively, were determined. Finally, the γ phase appears at 140 K and reaches saturation before the growth of multilayer NH_3, which indicates the presence of an additional NH_3 species that interacts in a weaker fashion with ZnO than multilayer NH_3.

An unambiguous identification of the surface NH_3-related species is provided by HREELS. Figure 2 b displays the temperature-dependent HREEL spectra recorded after exposing $ZnO(10\bar{1}0)$ to NH_3 at 100 K. The intense multiple-surface phonons (Fuchs–Kliewer modes) of ZnO (Figure 2 b, curve A) are completely removed by Fourier deconvolution (Figure 2 b, curve B), which allows us to observe the adsorbate-related losses. After NH_3 adsorption a number of new bands show up, indicating the existence of various NH_3-related species with different thermal stabilities, as demonstrated by the heating experiments (Figure 2 b, curves C–F and Table 1). Importantly, an OH band is clearly resolved at 3607 cm^{-1} for NH_3 adsorption at full ML, but disappears upon heating to 300 K, which corresponds to the desorption of the α_2 state in TDS (Figure 2 a). This finding is in excellent agreement with the IR results obtained on ZnO nanoparticles (Figure 1), thus revealing a reversible dissociation of NH_3 on $ZnO(10\bar{1}0)$ through hydrogen transfer with neighboring surface O^{2-} sites. After saturation of chemisorbed NH_3 at surface Zn^{2+} sites (α_2 and α_1 states), NH_3 can also interact weakly with the surface O^{2-} anion by NH···O hydrogen bonds, as characterized by the low-lying umbrella mode δ_s at 1060 cm^{-1},[18] which is stable only below 140 K (γ-NH_3). The multilayer NH_3 (β state) is identified by the δ_s and δ_{as} vibrations at 1158 and 1645 cm^{-1}, as well as by the broad band at 3393 cm^{-1}, which is assigned to the ν_{as}(N–H) mode of NH_3 within the H-bond network. In accord with the HREELS data on $ZnO(10\bar{1}0)$, both β- and γ-NH_3 species are also formed on ZnO nanoparticles (Figure 1).

To gain a thorough understanding of NH_3 chemistry on ZnO, and to elucidate the microscopic mechanism controlling hydrogen transfer on oxide surfaces, NH_3 adsorption on the $ZnO(10\bar{1}0)$ surface has been computationally investigated at different coverages: 0.125, 0.50, and 1.0 ML on a 4×2 surface supercell. In the low coverage regime, NH_3 molecules do not interact with their periodic images given a distance of 13.1 and 10.6 Å in the $[1\bar{2}10]$ and [0001] directions, respectively. The most stable configuration is a molecular adsorption structure (Figure 3 a) where the N atom coordinates through its lone pair electrons to a surface Zn^{2+} cation[19,20] and one H atom forms a hydrogen bond across the trench to a surface O^{2-} anion. The binding energy is 1.01 eV and the angle between the surface normal and the N–Zn axis is ca. 35°, which is in good agreement with experiment.[21] When the H-bonded proton is transferred to the binding surface O^{2-} anion to model NH_3 dissociation to NH_2, a spontaneous recombination is observed, as one would expect from the negligible acidity of this species. Dissociation leads to a stable intermediate

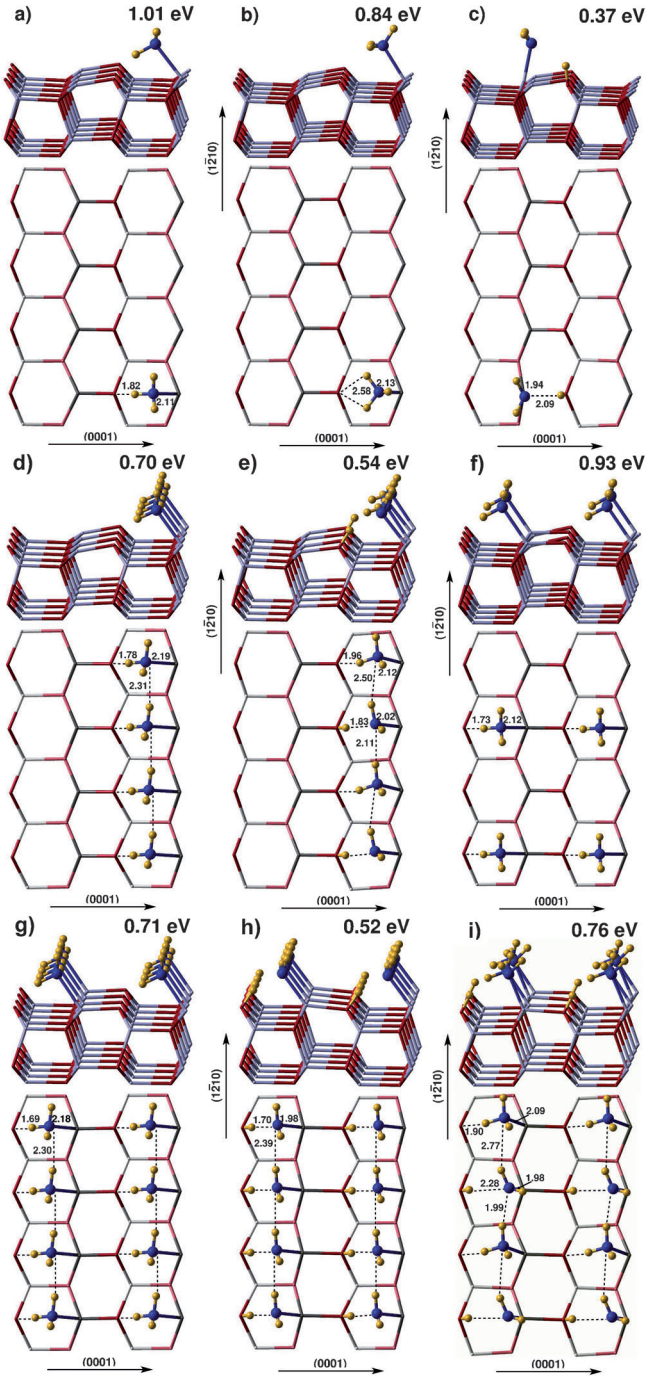

Figure 3. Front (upper portions) and top (lower portions) views of the main adsorption configurations and corresponding binding energies for: a–c) isolated NH_3 molecules (0.125 ML), d–f) NH_3 half coverage (0.50 ML), and g–i) NH_3 full coverage (1.0 ML) on the ZnO(10$\bar{1}$0) surface. Zn gray sticks, O red sticks (only two layers in the side view and one layer in the top view), N blue spheres, H yellow spheres. Distances are in Å.

(Figure 3c) only when the hydrogen is transferred to the low-coordinated O^{2-} directly bound to the adsorbing Zn^{2+} ion. This requires breaking of the Zn–O bond, and is energetically demanding. Bridging adsorption modes evolve into on-top ones.

At 0.5 ML coverage, molecular adsorption is still favored (Figure 3d–f), especially for a 2×1 superstructure with NH_3 molecules in rows along the [0001] direction (Figure 3f). This molecular array is 0.23 and 0.05 eV more stable than a row of adsorbates along the [1$\bar{2}$10] direction (Figure 3d) and a 2×2 zig-zag superstructure (Supporting Information, Figure S3), respectively. At half coverage ammonia dissociation becomes feasible in an alternating dissociated–undissociated configuration of rows along the [1$\bar{2}$10] direction, although it is still energetically rather costly (adsorption energy per molecule is 0.39 eV lower than for the molecular adsorption mode in Figure 3f). Partial dissociation in a row of molecules allows for the establishment of intermolecular H-bonding, which is otherwise prevented, and for the release of some steric repulsion. Dissociation across trenches, which is not observed at low coverage, is here induced by H-bonding with neighboring NH_3 molecules.

At full coverage the situation becomes unexpectedly different: the alternating dissociated–undissociated 2×1 superstructure (Figure 3i) is now the most stable by 0.05 eV, with respect to the fully undissociated configuration (Figure 3g). Translational symmetry between rows of alternating dissociated–undissociated molecules along the [1$\bar{2}$10] direction is found to favor partial dissociation (the 2×2 superstructure in Figure S4 is 0.39 eV less stable). The above two results provide clear evidence that the hydrogen transfer from non-acidic adsorbed molecular species to surface O^{2-} anions is induced by the high coverage, as a consequence of intermolecular H-bonding formation and the requirement for repulsion release.

With increasing coverage of molecular NH_3 on ZnO, adsorption energy decreases: when two molecules adsorb on neighboring Zn^{2+} sites along the [0001] and [1$\bar{2}$10] directions (0.25 ML coverage in Figure S2) a reduction of 0.04 and 0.10 eV is observed, respectively. The reason is that adsorbed molecular NH_3 is four-fold coordinated with no lone-pairs available for intermolecular H-bonding with neighboring molecules. This is fundamentally different from what happens for water molecules,[7] as we will discuss below.

The computed vibrational frequencies for stable NH_3 species at different coverages are summarized in Table 1. Overall, the calculated vibrational data and binding energies are in good agreement with measured results on the ZnO-(10$\bar{1}$0) surface. On the basis of the combined experimental and theoretical data for ZnO single-crystal surfaces, we can provide a consistent assignment of the IR bands observed on ZnO powder particles (Table 1). Exposure of polycrystalline ZnO powder to NH_3 at 100 K leads to its unexpected partial dissociation at full ML. This occurs predominantly on the perfect mixed-terminated ZnO(10$\bar{1}$0) surface by hydrogen transfer from adsorbed NH_3 to the adjacent O^{2-} base sites, as demonstrated by the coexistence of NH_3, NH_2, and isolated OH species. This partial dissociation gives rise to a (2×1) superstructure (Figure 3i), which corresponds to the α_2 state in the TD spectra. After heating to higher temperatures, the IR bands related to NH_2 and OH decrease significantly in intensity, revealing the back-transfer of released hydrogen to the NH_2 group at low coverage. At submonolayer coverage, NH_3 prefers to adsorb as an intact molecule (Figure 3a,f) at

Table 1: Experimental and calculated vibrational frequencies (in cm^{-1}) for ammonia at different coverages in the most stable configuration.

	Vibr. Mode	Experiment		Theory	
		IR	HREELS		
Low coverage: Isolated undissociated molecules (Figure 3 a)					
	ν_{Zn-N}	–	384	360	
	δ_s	1208	1190	1213	
	δ_a	1607	1610	1603	
NH_3		1632		1655	
	ν_s	–	–	2966	
	ν_{as}	3359	3407	3358	
		3410		3427	
High Coverage: Full monolayer				Undiss. (Figure 3 g)	Half-diss. (Figure 3 i)
	ν_{Zn-N}	–	384	287	379
	δ_s	1180	1175	1220	1219
NH_3	δ_a	1573	1624	1597	1599
		1622		1678	1682
	ν_s	3164	–	3375	3032
	ν_{as}	3413	3407	3458	3404
	ν_{Zn-N}	–	–	–	480
NH_2	δ	1542	1544	–	1513
	ν_s	3287	–	–	3324
	ν_{as}	3315	–	–	3374
OH	ν	3607	3607	–	3627

the surface Zn^{2+} site with a higher binding energy (α_1-NH_3). In addition to the majority of OH groups formed on ZnO(10$\bar{1}$0), the UHV-FTIRS data (Figure 1) show a weak band at 3621 cm^{-1}, which is stable at rather high temperatures and disappears only after heating to 800 K (Figures S5 and S6). This band is characteristic of OH species formed on the polar O-terminated ZnO(000$\bar{1}$) surface,[14,15] and indicates a dissociative adsorption of NH_3 at O vacancy sites on O–ZnO by hydrogen transfer to the neighboring surface O sites.

In Table 2 we compare binding energies for different adsorbates in different binding modes at low (0.125 ML) and full coverage (1 ML). From these data clear trends emerge that provide a solid basis for general consideration of the factors involved in the interaction of oxide surfaces with weak or extremely weak proton donors (Brønsted acids). The three adsorbates have increasingly high pK_a values; this indicates low, or even no, propensity for a hydrogen transfer to the surface, which is corroborated by a progressively lower binding energy for the dissociated form at low coverage. However, high surface coverage is capable of reversing the behavior of the adsorbates: hydrogen transfer to surface oxygen atoms is now energetically favored for 50% of the adsorbed molecules in an alternating undissociated–dissociated configuration, even in the case of NH_3, which normally acts as a base and not an acid. From the detailed analysis, three determining factors emerge: H-bonding, steric repulsion, and pK_a; water does not suffer much from steric repulsion, can establish H-bonding networks, and is the easiest to dissociate (lower pK_a). Therefore, adsorption energy increases at full coverage, especially for the half-dissociated configuration where stronger H-bonded dimers are formed. Methanol suffers from steric repulsion, lacks available protons for intermolecular H-bonding, and is only slightly less acidic than water. Therefore, binding energy decreases at full coverage, unless there is partial dissociation, which reduces repulsion and allows H-bonded dimer formation. Finally, ammonia is relatively bulky, lacks available N lone-pairs for H bonding, and, as a base, is definitely the least acidic. For these reasons, binding energies decrease at full coverage, with the partially dissociated configuration becoming unexpectedly favored thanks to the possibility of intermolecular H-bonding and release of steric repulsion.

Table 2: Binding energies (in eV) of different adsorbates on ZnO(10$\bar{1}$0) surface at different coverages.

Adsorbate	pK_a	Low coverage		High coverage	
		Undiss.	Diss.	Undiss.	Half-diss.
H_2O[7]	15.7	0.94	0.79	1.03	1.13
CH_3OH[22]	16	0.97	0.70	0.81	0.94
NH_3	35	1.01	0.37	0.71	0.76

In conclusion, our combined experimental and theoretical studies on ZnO surfaces of both single crystals and powder particles provide consistent evidence for the unusual partial dissociation of chemisorbed NH_3 on a perfect ZnO(10$\bar{1}$0) surface, which occurs only at full monolayer coverage through hydrogen transfer to the neighboring O^{2-} base sites, thus leading to the coexistence of NH_3, NH_2, and isolated OH groups in a (2×1) superstructure. The unambiguous fingerprint of this hydrogen transfer is an OH band (3607 cm^{-1}) observed for both single crystal and powder samples, and fully corroborated by theoretical calculations. This unexpected hydrogen transfer is triggered by a complex interplay between multiple factors including H-bonding, steric repulsion, and pK_a.

Experimental Section

The UHV-FTIRS experiments on polycrystalline ZnO powder samples (NanoTek, with a specific surface area of 14 $m^2 g^{-1}$) were performed in a novel UHV-FTIRS apparatus.[23,24] The powder samples were first pressed onto a stainless steel grid covered by gold and then mounted on a special sample holder to allow for the recording of FTIR data in a transmission geometry. The grid and the attached powder particles were cleaned in the UHV chamber by heating them to 700 K to remove all contamination. All UHV-FTIR spectra were collected with 1024 scans at a resolution of 4 cm^{-1} in transmission mode.[14] HREELS and TDS experiments on ZnO(10$\bar{1}$0) were carried out in a UHV apparatus that has previously been described in detail.[25] The single-crystal ZnO(10$\bar{1}$0) surface was cleaned by repeated cycles of sputtering (1 keV Ar^+, 30 min) and annealing in O_2 (1×10^{-6} mbar, 850 K, 2 min) and in UHV (850 K, 5 min). The surface purity was checked by LEED and HREELS.

Density functional theory calculations were carried out with the CRYSTAL09 code[26,27] using the B3LYP hybrid functional.[28,29] To model the mixed-terminated ZnO(10$\bar{1}$0) surface we used a periodically repeated slab of eight atomic layers with a (4×2) surface cell. The 2D irreducible Brillouin zone was sampled by four k points. Adsorption energies include the counterpoise correction for the basis set superposition error (BSSE). Vibrational frequencies at the Γ point were computed within the harmonic approximation on the optimized geometries by diagonalizing the mass-weighed Hessian matrix.

Received: September 18, 2012
Published online: January 7, 2013

Keywords: ammonia · density functional calculations · hydrogen transfer · oxides · vibrational spectroscopy

[1] S. C. Li, L. N. Chu, X. Q. Gong, U. Diebold, *Science* **2010**, *328*, 882 – 884.
[2] M. A. Henderson, *Surf. Sci. Rep.* **2002**, *46*, 1 – 308.
[3] U. Diebold, *Surf. Sci. Rep.* **2003**, *48*, 53 – 229.
[4] C. Wöll, *Prog. Surf. Sci.* **2007**, *82*, 55 – 120.
[5] A. Vittadini, A. Selloni, F. P. Rotzinger, M. Grätzel, *Phys. Rev. Lett.* **1998**, *81*, 2954 – 2957.
[6] a) L. Giordano, J. Goniakowski, J. Suzanne, *Phys. Rev. Lett.* **1998**, *81*, 1271; b) L. Giordano, J. Goniakowski, J. Suzanne, *Phys. Rev. B* **2000**, *62*, 15406 – 15408; c) Y. D. Kim, R. M. Lynden-Bell, A. Alavi, J. Stulz, D. W. Goodman, *Chem. Phys. Lett.* **2002**, *352*, 318 – 322; d) R. Włodarczyk, M. Sierka, K. Kwapień, J. Sauer, E. Carrasco, A. Aumer, J. Gomes, M. Sterrer, H.-J. Freund, *J. Phys. Chem. C* **2011**, *115*, 6764 – 6774.
[7] a) B. Meyer, D. Marx, O. Dulub, U. Diebold, M. Kunat, D. Langenberg, C. Wöll, *Angew. Chem.* **2004**, *116*, 6809 – 6814; *Angew. Chem. Int. Ed.* **2004**, *43*, 6641 – 6645; b) B. Meyer, H. Rabaa, D. Marx, *Phys. Chem. Chem. Phys.* **2006**, *8*, 1513 – 1520.
[8] S. Wendt, J. Matthiesen, R. Schaub, E. K. Vestergaard, E. Lægsgaard, F. Besenbacher, B. Hammer, *Phys. Rev. Lett.* **2006**, *96*, 066107.
[9] D. Marx, M. E. Tuckerman, J. Hutter, M. Parrinello, *Nature* **1999**, *397*, 601 – 604.
[10] O. Dulub, B. Meyer, U. Diebold, *Phys. Rev. Lett.* **2005**, *95*, 136101.
[11] Y. Du, N. A. Deskins, Z. Zhang, Z. Dohnálek, M. Dupuis, I. Lyubinetsky, *Phys. Rev. Lett.* **2009**, 102, 096102.
[12] G. Ertl, *Angew. Chem.* **2008**, *120*, 3578 – 3590; *Angew. Chem. Int. Ed.* **2008**, *47*, 3524 – 3535.
[13] H. J. Freund, G. Meijer, M. Scheffler, R. Schlögl, M. Wolf, *Angew. Chem.* **2011**, *123*, 10242 – 10275; *Angew. Chem. Int. Ed.* **2011**, *50*, 10064 – 10094.
[14] H. Noei, H. Qiu, Y. Wang, E. Löffler, Ch. Wöll, M. Muhler, *Phys. Chem. Chem. Phys.* **2008**, *10*, 7092 – 7097.
[15] H. Qiu, B. Meyer, Y. Wang, Ch. Wöll, *Phys. Rev. Lett.* **2008**, *101*, 236401.
[16] H. Wilmer, M. Kurtz, K. V. Klementiev, O. P. Tkachenko, W. Grünert, O. Hinrichsen, A. Birkner, S. Rabe, K. Merz, M. Driess, Ch. Wöll, M. Muhler, *Phys. Chem. Chem. Phys.* **2003**, *5*, 4736 – 4742.
[17] B. Meyer, D. Marx, *Phys. Rev. B* **2003**, *67*, 035403.
[18] Y. Wang, K. Jacobi, W.-D. Schöne, G. Ertl, *J. Phys. Chem. B* **2005**, 109, 7883 – 7893.
[19] M. Casarin, C. Maccato, A. Vittadini, *Chem. Phys. Lett.* **1999**, *300*, 403 – 408.
[20] N. H. Moreira, G. Dolgonos, B. Aradi, A. L. da Rosa, T. Frauenheim, *J. Chem. Theory Comput.* **2009**, *5*, 605 – 614.
[21] K. Ozawa, K. Edamoto, *Surf. Rev. Lett.* **2002**, *9*, 717 – 722.
[22] J. Kiss, D. Langenberg, D. Silber, F. Traeger, L. Jin, H. Qiu, Y. Wang, B. Meyer, Ch. Wöll, *J. Phys. Chem. A* **2011**, *115*, 7180 – 7188.
[23] Y. Wang, A. Glenz, M. Muhler, Ch. Wöll, *Rev. Sci. Instrum.* **2009**, *80*, 113108.
[24] M. Xu, H. Noei, K. Fink, M. Muhler, Y. Wang, C. Wöll, *Angew. Chem.* **2012**, *124*, 4810 – 4813; *Angew. Chem. Int. Ed.* **2012**, *51*, 4731 – 4734.
[25] Y. Wang, K. Jacobi, G. Ertl, *J. Phys. Chem. B* **2003**, *107*, 13918 – 13924.
[26] R. Dovesi, R. Orlando, B. Civalleri, C. Roetti, V. R. Saunders, C. M. Zicovich-Wilson, *Z. Kristallogr.* **2005**, *220*, 571 – 573.
[27] R. Dovesi, V. R. Saunders, C. Roetti, R. Orlando, C. M. Zicovich-Wilson, F. Pascale, B. Civalleri, K. Doll, N. M. Harrison, I. J. Bush, P. D'Arco, M. Llunell, *CRYSTAL09 (CRYSTAL09 User's Manual)*; University of Torino: Torino, **2009**.
[28] A. D. Becke, *J. Chem. Phys.* **1993**, *98*, 5648 – 5652.
[29] C. Lee, W. Yang, R. G. Parr, *Phys. Rev. B* **1988**, *37*, 785 – 789.

